Journal of Biomolecular NMR, 4 (1994) 61–78
ESCOM

J-Bio NMR 150

Backbone dynamics of ribonuclease T1 and its complex with 2'GMP studied by two-dimensional heteronuclear NMR spectroscopy

David Fushman, Rüdiger Weisemann, Harald Thüring and Heinz Rüterjans*

Institut für Biophysikalische Chemie der Johann-Wolfgang Goethe Universität Frankfurt am Main, Theodor-Stern Kai 7, Haus 75A, D-60590 Frankfurt am Main, Germany

Received 20 April 1993
Accepted 3 August 1993

Keywords: 2D heteronuclear NMR; Protein dynamics; Order parameter; Ribonuclease T1; Inhibitor complexes

SUMMARY

The backbone dynamics of free ribonuclease T1 and its complex with the competitive inhibitor 2'GMP have been studied by ^{15}N longitudinal and transverse relaxation experiments, combined with $\{^1H,^{15}H\}$ NOE measurements. The intensity decay of individual amide cross peaks in a series of $(^1H,^{15}N)$-HSQC spectra with appropriate relaxation periods (Kay, L.E. et al. (1989) *Biochemistry*, **28**, 8972–8979; Kay, L.E. et al. (1992) *J. Magn. Reson.*, **97**, 359–375) was fitted to a single exponential by using a simplex algorithm in order to obtain ^{15}N T_1 and T_2 relaxation times. These experimentally obtained values were analysed in terms of the 'model-free' approach introduced by Lipari and Szabo (Lipari, G. and Szabo, A. (1982) *J. Am. Chem. Soc.*, **104**, 4546–4559; 4559–4570). The microdynamical parameters accessible by this approach clearly indicate a correlation between the structural flexibility and the tertiary structure of ribonuclease T1, as well as restricted mobility of certain regions of the protein backbone upon binding of the inhibitor. The results obtained by NMR are compared to X-ray crystallographic data and to observations made in molecular dynamics simulations.

INTRODUCTION

It is well accepted now that the internal mobility of proteins is of utmost importance for their biochemical activity and function. Recent development of pulsed NMR, especially of its multidimensional versions, has made this method an effective tool for investigating the motion of particular molecular parts of proteins in order to gain insight into the relation between protein dynamics and biochemical activity. In previous studies (Kay et al., 1989, 1992; Clore et al., 1990a, b; Barbato et al., 1992; Redfield et al., 1992) a methodology based on NMR relaxation measurements has been developed to provide reasonable information on the internal dynamics of protein

*To whom correspondence should be addressed.

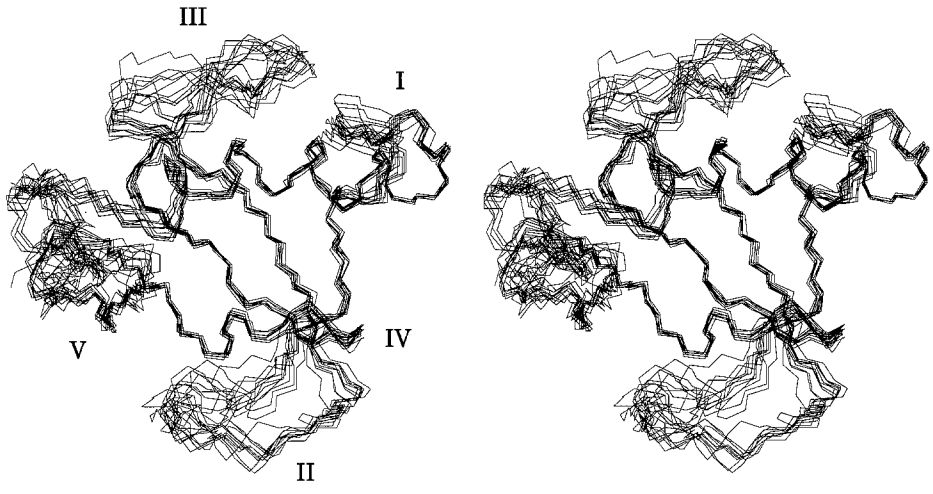

Fig. 1. Stereoview of the 13 best solution structures of RNase T1 obtained from NMR data using the distance geometry algorithm DIANA. The loop regions I to V are marked.

molecules in solution. In the present work these NMR relaxation methods are applied to investigate the molecular dynamics of ribonuclease T1. Ribonuclease T1 is a small globular endoribonuclease (104 amino acids, MW about 11 kDa) from the fungus *Aspergillus oryzae* which has been widely used as a model for nucleic acid–protein interactions as studied by X-ray crystallography (Heinemann and Saenger, 1982, 1983; Sugio et al., 1985, 1988; Arni et al., 1988a,b; Hakoshima et al., 1988; Heinemann and Hahn, 1989; Martinez-Oyanedel et al., 1991), NMR spectroscopy (Rüterjans et al., 1987; Hoffmann and Rüterjans, 1988; Schmidt et al., 1991) and several other biophysical and biochemical methods (Takahashi et al., 1967; Takahashi, 1970, 1976; Arata et al., 1976; Hakoshima et al., 1988). RNase T1 specifically cleaves single-stranded RNA at the 3' end of guanosine nucleotides. 3'- and 2'-guanosine monophosphates (GMP) act as competitive inhibitors of the enzyme (Egami and Sato, 1965). The tertiary structure of RNase T1 consists of a central five-stranded antiparallel β-sheet (residues 39–42, 56–61,75–81, 86–92, and 100–103), a short two-stranded β-sheet near the N-terminus (residues 4–11) and a peripheral regular α-helix (residues 13–29). These well-defined secondary structure elements are connected by loop or turn regions (residues 30–38 (Loop I), 43–55 (Loop II), 62–74 (Loop III), 82–85 (Loop IV), 93–99 (Loop V)), for which structure calculations based upon distance geometry and molecular dynamics methods indicate an intrinsic flexibility. Of these loop regions, especially Loop V is considered to be important for the binding of the substrate and the competitive inhibitors to ribonuclease T1. Nevertheless, the question whether the well-known picture of NMR-derived structures fanning out for disordered parts of the molecule (cf. Fig. 1) is really a matter of mobility or a lack of NOE constraints remains unanswered in most reported cases. One goal of the present study is therefore to analyse the backbone dynamics of free ribonuclease T1 with respect to the flexibility of the loop regions as apparent from distance geometry and molecular dynamics calculations and to compare these results to those obtained for an inhibitor complex of this enzyme, in order to assess possible changes in the mobility of those peptide segments of the protein that are known to be involved in substrate binding and the catalysis of RNA degradation.

MATERIALS AND METHODS

Sample preparation

Recombinant RNase T1 was isolated from the *E. coli* strain DH5α/pA2T1 harbouring the RNase T1 gene (Quaas et al., 1988a,b) following a procedure described by Schmidt et al. (1991). Uniform ^{15}N enrichment (> 99%) was achieved by growing the bacteria in a modified M9 medium containing $^{15}NH_4Cl$ (Isotech Inc., Miamisburg, Ohio, 99.7% atomic purity) as the sole nitrogen source.

Experimental conditions

All NMR experiments were performed on a Bruker AMX 600 spectrometer operating at 308 K. Ribonuclease T1 was diluted in 95%H_2O/5%D_2O to final concentrations of 2.0 mM for the ribonuclease T1/2'GMP complex and 3.0 mM for the uncomplexed ribonuclease T1, the pH being adjusted to 5.4. In order to ensure saturation of the protein with inhibitor, a 2.5-fold molar excess of 2'GMP was added to the protein in the case of the complexed sample. In all NMR experiments, the ^1H carrier frequency was set into the middle of the amide spectral region by using off-resonance presaturation with a series of weak phase-modulated square-shaped pulses, where appropriate. Spectral widths were set to 2000 Hz in the nitrogen dimension and 4500 Hz in the proton dimension, yielding a digital resolution of 1.95 Hz/point in the F_1 dimension and 2.2 Hz/point in the F_2 dimension after zero-filling and Fourier transformation. The spectra were processed and analysed on a Bruker X32 workstation using the programs UXNMR and AURELIA (Bruker Analytische Messtechnik GmbH, Karlsruhe).

T_1 and T_2 measurements

Longitudinal and transverse nitrogen relaxation times were measured by using the pulse sequences described by Kay et al. (1992), which were designed to eliminate the effect of cross-correlation between dipolar and chemical shift anisotropy relaxation mechanisms (see also Goldman, 1984; Boyd et al., 1990, 1991; Palmer et al., 1992). Series of six or seven 2D spectra were recorded in each experiment, with typical relaxation delays having been set to 14.4, 72.0, 144.0, 288.0, 432.0, 576.0 and 720.0 ms for the T_1 measurements, or 3.6, 28.8, 57.6, 86.4, 129.6 and 172.8 ms in the experiments designed to measure nitrogen transverse relaxation.

Nuclear Overhauser effect

In order to evaluate the $\{^1H\}$-^{15}N nuclear Overhauser effect on the amide nitrogen spin, 2D spectra were recorded with and without NOE enhancement by presaturation of the amide protons. ^1H presaturation in the experiment with NOE was achieved by applying 120° pulses, spaced at 20-ms intervals, for 3 s prior to the first ^{15}N pulse, the whole delay between successive scans being 5 s in both experiments, with and without NOE. To achieve effective water signal suppression, a ^1H spin-lock pulse of 4 ms duration was applied prior to the first 90° ^{15}N-pulse. In addition, a 90_x (^1H) pulse, to remove the antiphase component of the magnetisation, was used prior to acquisition.

Data evaluation

The amino acid sequence of RNase T1 consists of 104 residues, forming a single polypeptide

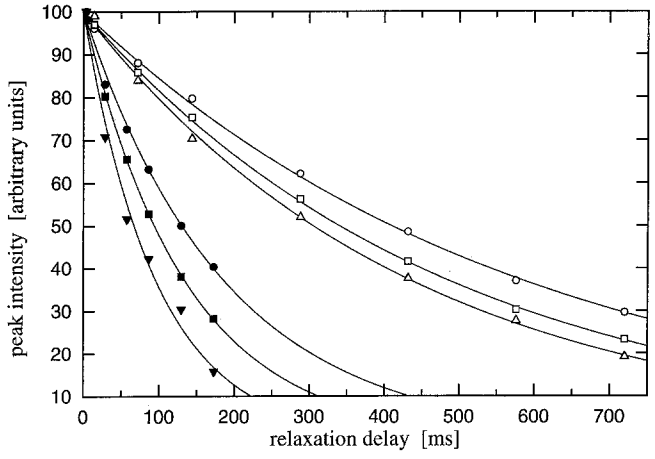

Fig. 2. Experimental and calculated intensity decay curves for Tyr^{24} (open triangles), Val^{78} (black triangles), Gly^{88} (squares) and Thr^{104} (circles). The symbols indicate the measured peak intensities in arbitrary units, whereas the curves were calculated using the amplitudes and time constants derived by the least-squares fit. Data is shown for T_1 and T_2 measurements, the open and solid symbols, respectively. The residues are chosen to present a slow, fast and some intermediate decay in each type of experiment.

chain of a total molecular mass of approximately 11 kDa. Assignments of the ^1H and ^{15}N resonances in RNase T1 and the RNase T1 · 2'GMP complex have been completed previously (Schmidt et al., 1990,1991; Werner, A., Karimi-Nejad, Y., Hoffmann, E., Simon, J., Thüring, H. and Rüterjans, H., unpublished results). In the present work, 92 and 83 sufficiently well-resolved cross peaks from amide NH groups have been used during the data evaluation in the case of the free enzyme and its complex with 2'GMP, respectively. The remaining resonances could be assigned in the recorded spectra, but their integral values proved to be unreliable due to spectral overlap or artifacts. ^{15}N longitudinal (T_1) and transverse (T_2) relaxation times were evaluated by fitting the intensity decay of corresponding resonances in the series of 2D spectra to a single exponential, depending on the relaxation delays. The data was fitted by a least-squares minimisation procedure based on a downhill-simplex algorithm (Press et al., 1988). Typical decay curves as well as their best fits are shown in Fig. 2.

Error estimation

The parameters obtained from the least-squares fit of an exponential decay, its amplitude (A_n) and time constant (T_n, n = 1 or 2) are prone to systematic experimental errors, which were evaluated by the following statistical procedure. Since the experimental errors are not known in advance, the standard deviation of the experimental data was derived from the residual of the fit, assuming that all points in the T_1 or T_2 curves have the same standard deviation. The validity of this assumption could be shown by evaluation of the noise level in the 2D spectra, which turned out to be approximately the same for all the time points in the series. In the next step, the standard deviation of the fitting parameters was obtained by a Monte Carlo approach by using either the method of constant chi-square boundaries (Press et al., 1988) or simulated experimental data as described by Kamath et al. (1989) and Nicholson et al. (1991). Briefly, the first method is based

on random perturbations of the fitting parameters around their best-fit values in order to determine a confidence region with a defined increase in the chi-square value describing the goodness of fit. In the second method, several sets of 'experimental' data are synthesized by using random numbers with standard deviations as determined above, and a distribution of parameters (A_i, T_i) giving the best fit to each simulated data set is analysed statistically. For both methods, 500 statistical events were analysed. To estimate the experimental error in the measured NOE enhancement, the standard deviation of the baseline noise was determined for each 2D experiment by integration of empty regions of the spectra. The error associated with the NOE value for a certain cross peak was calculated by:

$$\sigma_{NOE} = \{I_A/I_B\} \sqrt{\{(\delta I_A/I_A)^2 + (\delta I_B/I_B)^2\}} \quad (1)$$

where I and δI denote the intensity of the peak and its standard deviation, respectively, and subscripts A and B refer to spectra recorded in the presence and absence of NOE enhancement, respectively.

Three independent T_1-, two T_2-, and three NOE measurements were performed for the RNase T1 · 2'GMP complex. In this case, the values of the parameters obtained from different measurements were averaged to yield the actual values of T_1, T_2, and NOE for a further analysis. The error values from each set of measurements and the standard deviation obtained in the course of averaging were compared, the largest one being taken as an estimate of the standard deviation of the corresponding parameter.

Spin relaxation and the model of motion

The dynamical parameters of ribonuclease T1 were evaluated from experimentally obtained ^{15}N T_1, T_2 and NOE values by using standard expressions (Abragam, 1961; Lipari and Szabo, 1982). The interactions that were taken into account for the nuclear spin relaxation of the amide nitrogen under consideration are the ^{15}N chemical shift anisotropy (CSA) and the dipole–dipole interaction between the amide nitrogen and its directly bound hydrogen. The relevant correlation function of the N–H bond reorientations is taken as a product of the corresponding correlation functions describing the overall tumbling of the protein, $C_R(t) = 0.2 \exp(-t/\tau_c)$, and the internal motions, $C_i(t)$. The form of $C_i(t)$, used in most cases in the present work, is the one introduced by Lipari and Szabo (LS) (1982) within the so-called 'model-free' approach, representing the decay of the correlation of internal motion by a one-exponential process:

$$C_i(t) = S^2 + (1 - S^2) \exp\left(\frac{-t}{\tau_l}\right) \quad (2)$$

In this approach, the internal dynamics is described in terms of the correlation time τ_l, which is assumed to be much shorter than the correlation time of overall tumbling, τ_c, and the order parameter S characterizing the amplitude of local motion: S equals 1 for completely restricted motion, while S equals 0 for unrestricted internal reorientations. All calculations were performed under the assumption of isotropic overall tumbling of the protein, which may be inferred from the ratio of the three principal components of the inertia tensor as calculated from X-ray crystallographic data: 1:1.14:1.27 for the free enzyme and 1:1.12:1.25 in the case of the RNase T1 · 2'GMP complex (Arni et al., 1988a,b; Martinez-Oyanedel et al., 1991).

In the course of analysis (see below) for some of the residues the simple form of Eq. 2 turned out to be insufficient to agree with the whole set of experimental data. In these cases a modified Lipari-Szabo approach (Clore et al., 1990a) was used to evaluate the parameters:

$$C_i(t) = S^2 + (S^2_{fast} - S^2) \exp\left(\frac{-t}{\tau_{slow}}\right) + (1 - S^2_{fast}) \exp\left(\frac{-t}{\tau_{fast}}\right) \quad (3)$$

In this biexponential representation the subscript 'fast' refers to the motions on a time-scale much faster than τ_c, while 'slow' denotes the parameters of internal motion in a time window comparable to the time of overall protein rotation, and $S^2 = S^2_{slow}S^2_{fast}$ has the same meaning as in Eq. 2.

Evaluation of microdynamical parameters

The microdynamical parameters, τ_c, S^2 and τ_l were derived from the minimisation of the following target function:

$$\chi^2 = \sum_{k=1}^{N} \left\{ \frac{(T^o_{1k} - T^c_{1k})^2}{\sigma^2_{1k}} + \frac{(T^o_{2k} - T^c_{2k})^2}{\sigma^2_{2k}} + \frac{(NOE^o_k - NOE^c_k)^2}{\sigma^2_{NOEk}} \right\} \quad (4)$$

where the sum runs over all the residues σ_{1k}, σ_{2k}, and σ_{NOEk} are standard deviations in T_1, T_2 and NOE for the *k*th residue, respectively, and superscripts 'o' and 'c' refer to observed and calculated values of the relaxation parameters. The overall tumbling time, τ_c, was changed stepwise being taken to be the same for all the residues, while the parameters of internal motion varied from one residue to the other. The confidence limits of the microdynamical parameters derived during this minimisation were obtained by the method of constant chi-square boundaries described above, with the acceptance condition of a minimum of 250 points within the confidence region.

Since T_2 values observed in CPMG-type experiments (Carr and Purcell, 1954; Meiboom & Gill, 1958) may be subject to an apparent shortening due to processes of conformational or chemical exchange on time scales smaller than or comparable to the delay between successive 180° pulses, thereby contributing to the measured transverse relaxation rate (Bloom et al., 1965; Kay et al., 1989), not all the measured T_2 values may be used for the evaluation of Eq. 4. To determine the exchange contributions to the apparent transverse relaxation rate of individual nitrogen spins, a 'selection criterion' based on the analysis of (T_1/T_2) ratios was applied (Clore et al., 1990a). Following this criterion, eight amide groups in the free enzyme and nine in the inhibitor complex showed (T_1/T_2) ratios more than one standard deviation larger than the mean value ($< T_1/T_2 >$) and hence are influenced by chemical exchange processes. For these residues only T_1 and NOE data were used for the estimation of the dynamical parameters. After calculation of these parameters, the expectation value of transverse relaxation time, T^c_2, was calculated, and the contribution of the exchange processes to the measured relaxation rate was given by:

$$R_{ex} = \frac{1}{T^o_2} - \frac{1}{T^c_2} \quad (5)$$

On the other hand, (T_1/T_2) ratios more than one standard deviation below the mean value indicate the presence of local motions on a time-scale comparable to the time of overall tumbling. Eleven amide groups in the free enzyme and seven in the complex, mainly being located in

unstructured regions of the protein, showed this behaviour. For these residues both the LS and modified LS approaches (Eqs. 2 and 3, respectively) were applied. Since only three experimental parameters are available for each nitrogen nucleus, the system is underestimated for the application of the modified LS model. To avoid this difficulty, the number of fitting parameters was reduced to three (S^2, S^2_{fast} and τ_{slow}), letting $\tau_{fast} = 0$ and taking τ_c as obtained from the minimisation of χ^2, Eq. 4, using the LS model. However, the changes in χ^2 upon using Eq. 3 instead of Eq. 2 appeared to be insignificant in some analysed cases. In summary, the application of the modified LS model seems to be appropriate for the following residues: Gly^7, Ser^{53}, Tyr^{56}, Ser^{63}, Gln^{85}, His^{92}, Gly^{97}, Asn^{99}, and Thr^{104} in free RNase T1, and Phe^{50} and Val^{52} in the RNase T1 · 2'GMP complex.

Note that, using the (T_1/T_2) ratios which fall within one standard deviation of the mean, the overall rotational correlation time can be estimated by:

$$\tau_c = \frac{1}{2\omega_N} \times \sqrt{\frac{6T_1}{T_2} - 7} \tag{6}$$

which is valid for short τ_l values ($\tau_l < 100$ ps) and $S^2 > 0.5$, ω_N being the Larmor frequency of ^{15}N. The values of τ_c thus derived, 5.27 ± 0.18 ns (free RNase T1) and 4.63 ± 0.18 ns (RNase T1 · 2'GMP) are in good agreement with those obtained from a more detailed analysis (see below).

Chemical exchange contribution to the linewidth

The chemical exchange contribution to the apparent T_2 values observed experimentally is attributed to random fluctuations of the Larmor frequency during the periods of free precession (Bloom et al., 1965; Kay et al., 1989), due to reasons other than an ordinary rotational modulation of the dipole–dipole interaction in the N–H pair and the ^{15}N CSA, already taken into account in the evaluation of the ^{15}N linewidth. Chemical exchange in this context is used to summarise contributions of both exchange between different conformations and hydrogen exchange processes involving the amide proton.

Using Anderson's exchange model between two sites with Larmor frequencies $+\delta$ and $-\delta$ (Anderson, 1954) and the exchange rate K, it is easy to show (Bloom et al., 1965) that in the extreme narrowing regime ($K \gg \delta$), which is reasonable in the case under consideration, the exchange contribution to the observed transverse relaxation rates depends on the relation between K and the time constant ξ in the CMPG sequence: for $K\xi \ll 1$ it has practically no effect on T_2, while in the case of $K\xi \gg 1$ (long ξ-fast exchange limit; Bloom et al., 1965) it is given by:

$$R_{ex} = \frac{\delta^2}{2K} \tag{7}$$

Although the real picture of chemical exchange in macromolecules may be more complicated than this simple model, this equation can be used to analyse the effects of conformational exchange on the results of the CPMG-type T_2 measurements to a first-order approximation. Depending on the repetition delay in the modified CPMG pulse train (Kay et al., 1992), $2\xi = 900$ μs in the present study, only exchange processes occurring at a rate of 10^3 s^{-1} or faster can be expected to show a significant influence on the measured T_2 values.

RESULTS AND DISCUSSION

Relaxation data and dynamical parameters

The ^{15}N longitudinal and transverse relaxation times as well as the NOEs derived from the 2D spectra are presented in Figs. 3 (free enzyme) and 4 (inhibitor complex). It is obvious from the data that the average level of the T_1 values in the free RNase T1 is higher than in the RNase T1 · 2'GMP complex, while the behaviour of the T_2 values is opposite. Therefore the mean (T_1/T_2) ratio for the free enzyme is larger, and from Eq. 6 a longer overall rotational correlation time is expected. τ_c therefore was 5.30 ± 0.13 ns for RNase T1 and 4.70 ± 0.10 ns for RNase T1 · 2'GMP. The difference in the τ_c reflects different protein concentrations and hence different solution viscosities in both samples. The values obtained by the NMR approach are well within the range of correlation times of RNase T1 obtained from fluorescence decay measurements (Eftnik, 1983; Lakowicz et al., 1983; James et al., 1985; Chen et al., 1987).

Physical insight into the influence of the local motion on the ^{15}N spin relaxation rates in the LS model can be easily obtained if one writes, using Eq. 2:

$$\frac{1}{T_n} = \frac{1}{T_n^{iso}(\tau_c)} - (1 - S^2)\left\{\frac{1}{T_n^{iso}(\tau_c)} - \frac{1}{T_n^{iso}(\tau_e)}\right\}, \qquad n = 1, 2 \tag{8}$$

with $1/T_n^{iso}(\tau_c)$ and $1/T_n^{iso}(\tau_e)$ denoting the corresponding relaxation rates calculated for the case of purely isotropic rotational motion with correlation times τ_c and τ_e, respectively, and τ_e being defined by: $\tau_e^{-1} = \tau_c^{-1} + \tau_l^{-1} \cong \tau_l^{-1}$. In the case of transverse relaxation, the expression in curly brackets on the righthand side of Eq. 8 is always positive, due to the monotonous increase of $1/T_2^{iso}(\tau)$ versus τ. Hence, the presence of local anisotropic motion always leads to an increase in T_2. A similar conclusion can be made for the longitudinal relaxation, despite the non-monotonous behaviour of $1/T_1^{iso}(\tau)$ versus τ, since under conventional experimental conditions the values of τ_c are near or only slightly above the value of $1/\omega_N$, at which $1/T_1^{iso}(\tau)$ as a function of τ reaches its maximum, whereas τ_e is supposed to be considerably shorter than τ_c. Thus, the presence of local anisotropic motion in a protein always leads to a shortening of the corresponding ^{15}N relaxation rates, proportional to the value of $1 - S^2$.

The residues with higher amplitude of internal motion should have simultaneously higher values of T_1 and T_2. On the other hand, amide groups with the lowest values of T_1 and T_2 belong to the residues with the most restricted local mobility. Note that in the latter case only the values of T_1 may be taken for a reliable analysis, because of the shortening of the T_2 values due to chemical exchange.

Before discussing the values of microdynamical parameters derived from the measured relaxation rates, the sensitivity of the latter to S^2 and τ_l should be evaluated. In Fig. 5, contour plots are shown of $1/T_1$, $1/T_2$, and NOE in the coordinates S^2 and τ_l. The calculation details are given in the caption of Fig. 5. From these pictures, it is obvious that in the region $S^2 > 0.5$, $\tau_l < 100$ ps, which is important for the internal dynamics of a protein detected by NMR at high fields, the rates of longitudinal and transverse relaxation are almost insensitive to the time constant of local motion, τ_l. While knowledge of only one of the relaxation parameters may be quite sufficient to determine S^2 in this region, provided the overall correlation time τ_c is known, the values of both T_1 and T_2 are not sufficient for correct calculation of τ_l, since small errors in these parameters may lead to a large uncertainty in the evaluation of the latter. For a more reliable determination of τ_l,

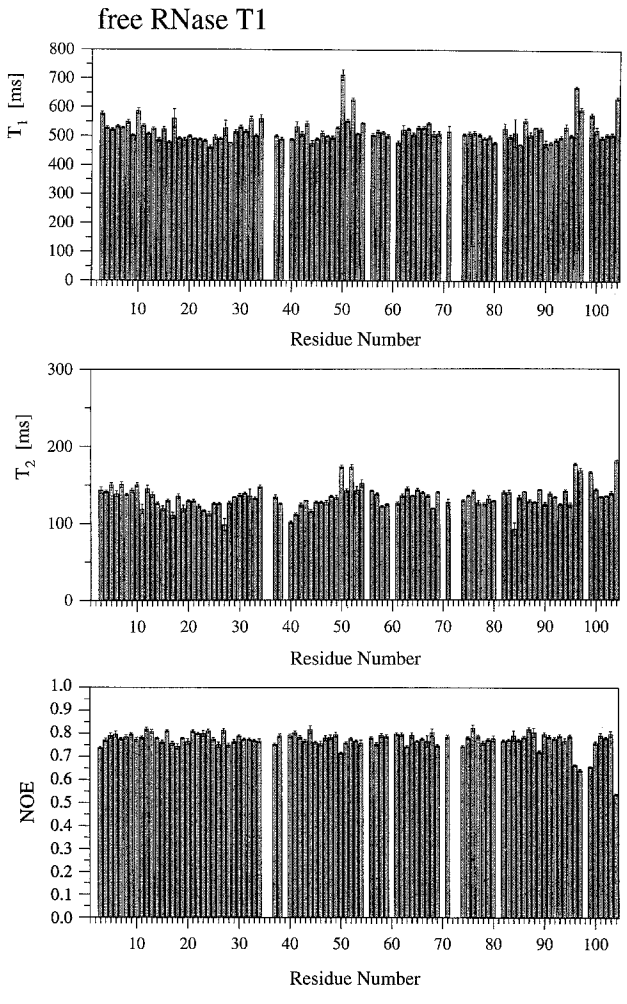

Fig. 3. Experimental T_1, T_2 and $\{^1H,^{15}N\}$ NOE values for free ribonuclease T1 as a function of residue number.

information about the NOE enhancement is necessary, although it cannot lead to a drastic reduction in the error of the τ_i values, because of the small gradient of the NOE profile in the above-mentioned region. Therefore in the further analysis we concentrate mainly on the order parameter values.

Free ribonuclease T1

Figure 6 shows the order parameter distribution obtained for the free enzyme by NMR and the temperature B-factors of the backbone nitrogen atoms extracted from the crystal structure of free ribonuclease T1 (Martinez-Oyanedel et al., 1991). To allow for a direct comparison with the X-ray data, $(1 - S^2)$, being the deviation of S^2 from its complete restriction-limit value and therefore increasing with the increase in the amplitude of local motion, is plotted versus the amino acid sequence.

From Fig. 6, differences in the internal mobility are obvious for the regions of regular second-

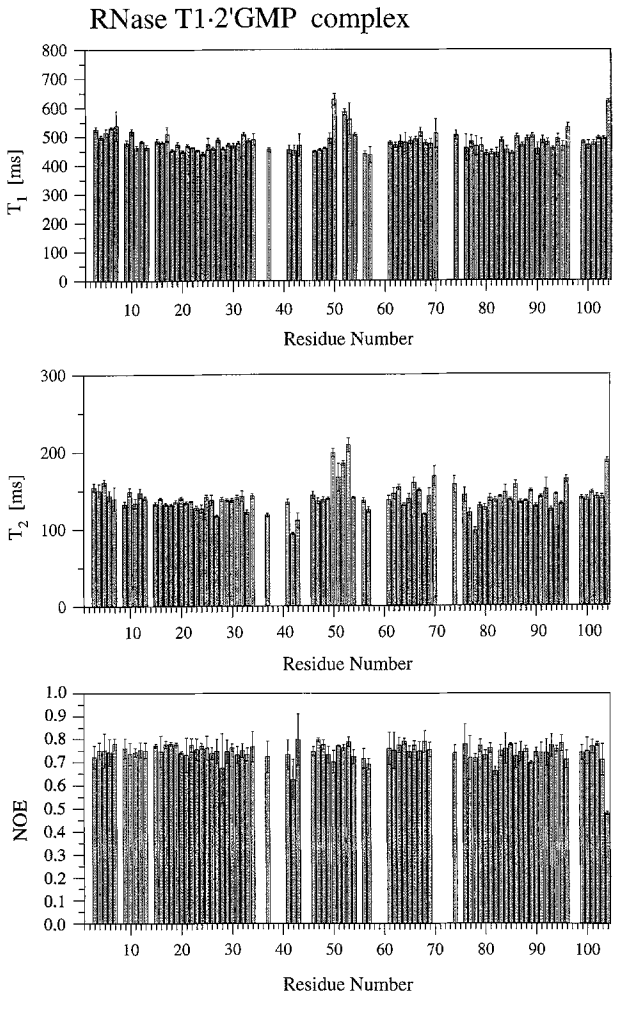

Fig. 4. Experimental T_1, T_2 and $\{^1H,^{15}N\}$ NOE values for the ribonuclease T1 · 2'GMP complex as a function of residue number.

ary structure and the disordered structure elements. The smallest amplitudes of local motion ($1 - S^2$ below 0.14) were obtained for the residues belonging to the peripheral α-helix (residues 13 to 29) and for the residues belonging to the strands of the central anti-parallel β-sheet (residues 40–42, 56–61, 75–81, 86–92 and 100–103) of RNase T1, thus indicating highly restricted local mobility of these parts of the protein backbone. It is worth noting here that the lowest amplitude of internal motion ($1 - S^2$ about 0.02) was observed for Tyr^{24}, which has the shortest T_1 value (cf. the discussion following Eq. 8). The local mobility of the loop regions as well as that of the termini is less restricted, as follows from rather high values of $1 - S^2$, up to 0.33–0.35 for Phe^{50}, Ser^{96} and Thr^{104}. If, for example, the 'wobbling-in-a-cone' model is used for the motion of the N–H bond vector, i.e., $S = 0.5 \cos\alpha\,(1 + \cos\alpha)$, with α being the semi-angle of a cone of all possible orientations of the N–H bond, the values of the semi-angle range from 7° to 18° for residues within a regular secondary structure and up to about 30° for residues belonging to loop regions.

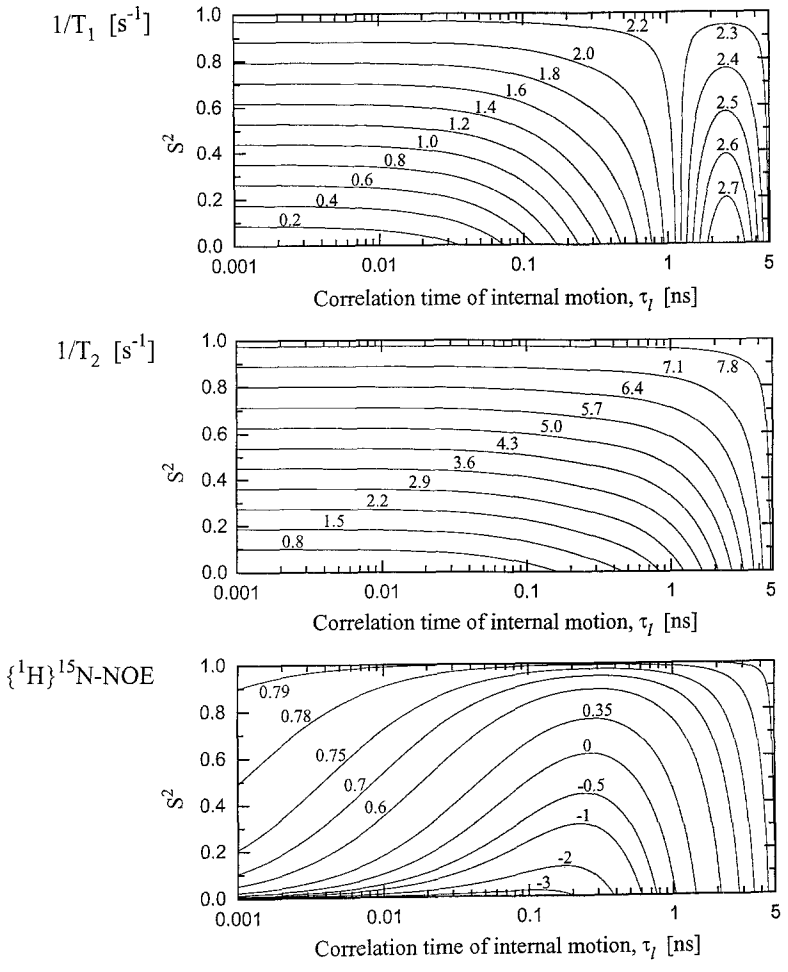

Fig. 5. Contour plots of the theoretical dependence of $(T_1)^{-1}$, $(T_2)^{-1}$ and $\{^1H,^{15}N\}$ NOE values on the square of the order parameter (S^2) and on the correlation time of internal motion (τ_I), calculated using the Lipari and Szabo model, Eq. 2. An overall rotation correlation time of 5 ns was used in the calculations at Larmor frequencies of 600.13 MHz for ^1H and 60.81 MHz for ^{15}N. An average N–H bond length of 0.102 nm and a constant ^{15}N CSA of −160 ppm (Hiyama et al., 1988) were assumed in all calculations.

RNase T1 · 2'GMP complex

The distribution of the amplitudes of local motion for this sample is similar to the one obtained for the free enzyme, as is evident from the Fig. 7, where the distribution of the atomic B-factors derived from the crystal structure of the RNase T1 · 2'GMP complex (Arni et al., 1988a,b) is also presented. Order parameter values for the residues belonging to structured parts of the backbone fall in the same range as in free RNase T1. The main changes in local mobility, compared to the free enzyme, were observed in the loops II and V, namely an increase in the amplitude of internal motion of residues 50–53 and a decrease in the mobility of residues 96–99 and 100. The apparent changes in loop II cannot be attributed to inhibitor binding or catalytic activity in a straightforward manner, since these residues are not known to take part in the biochemical activity of

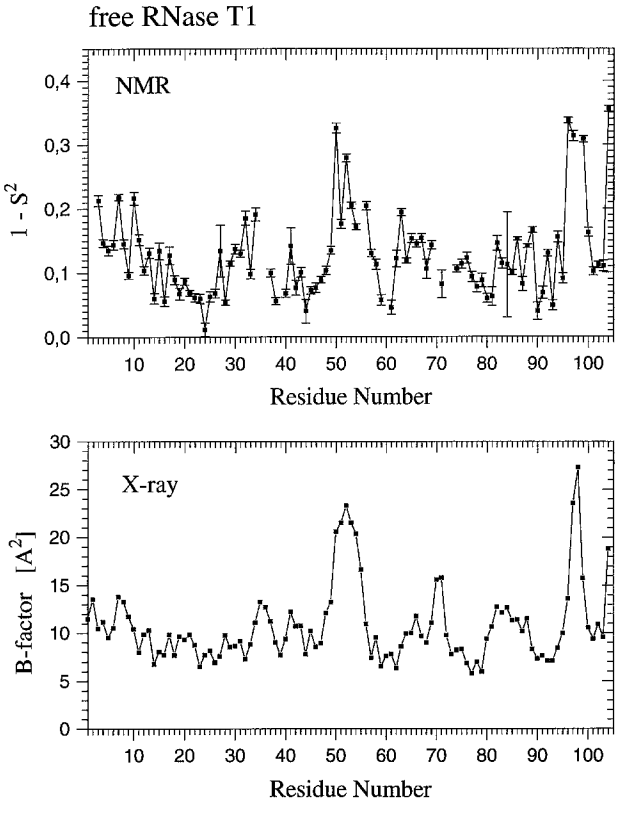

Fig. 6. Free RNase T1: the calculated $1 - S^2$ values (see text) and temperature B-factors of the amide nitrogens (from the crystal X-ray data, Martinez-Oyanedel et al., 1991).

ribonuclease T1, whereas the changes in loop V can be attributed to inhibitor binding, as inferred from X-ray studies (Heinemann and Saenger, 1982; Arni et al., 1988a,b) and recent NMR investigations (Werner, A., Karimi-Nejad, Y., Hoffmann, E., Simon, J., Thüring, H. and Rüterjans, H., unpublished results). From these studies, it is known that the backbone carbonyl function of Asn^{98} forms a hydrogen bond with the exocyclic amino group of the guanine base, while the backbone amide group of Asn^{98} forms a part of a RNase T1 subsite (Steyaert et al., 1991). Phe^{100} is also involved in the binding site: its amide proton participates in hydrogen bonding to the Glu^{46} side chain carbonyl group, while the side chain of Phe^{100} is oriented towards the base. The backbone mobility for the neighbouring residues, especially for the Asn^{99} NH group belonging to the same peptide plane as Asn^{98} CO, should be influenced by inhibitor binding due to secondary processes. It is worthwhile mentioning that according to X-ray data the Asn^{99} side chain in free RNase T1 adopts two conformations, in contrast to only one in the RNase T1 · 2'GMP complex (Martinez-Oyanedel et al., 1991).

To illustrate the decrease in mobility of the loop V region upon binding of the inhibitor, the difference in the S^2 values for residues 92–104 in the RNase T1 · 2'GMP complex and in free RNase T1 is depicted in Fig. 8. Unfortunately, the lack of some important experimental data (Asn^{98} ^{15}NH cross peak has not been assigned in both samples and the data for the Asn^{97} ^{15}NH

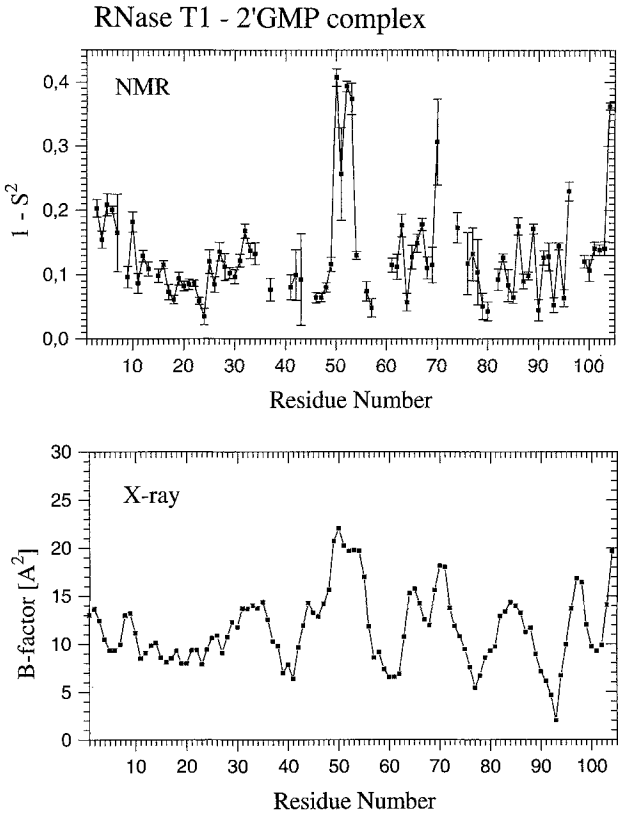

Fig. 7. RNase T1 · 2'GMP complex: the calculated $1 - S^2$ values and temperature B-factors of the amide nitrogens (from the crystal X-ray data, Arni et al., 1988a).

signal in the complexed sample proved unreliable during data evaluation) does not allow for a detailed comparison of the dynamic parameters and the corresponding B-factors. However, the increase in the order parameter (decrease of $1 - S^2$) in this region for the RNaseT1 · 2'GMP complex compared to the free RNase T1 indicates a real motional restriction. This follows from the noticeable simultaneous increase in T_1 and T_2 values and decrease in NOE for the corresponding residues in free enzyme which were not observed in the RNase T1 · 2'GMP complex, as can be clearly seen from the comparison of Figs. 3 and 4.

Chemical exchange

Using Eq. 5, values for the contribution of chemical exchange, R_{ex}, to the transverse relaxation of several ^{15}N nuclei, that exhibited an increase in the transverse relaxation rate of more than 1 s^{-1} in at least one of the samples, were obtained and are presented in Table 1. Of these residues, His^{40}, Glu^{58}, and Arg^{77} belong to the catalytic site of RNase T1, while the residues 41–44 are known to be involved in the recognition of the base moiety, with the amide groups of Asn^{43} and Asn^{44} directly participating in hydrogen bonding with the guanine base, according to X-ray (Heinemann and Saenger, 1982) and transient NOE data (Werner, A., Karimi-Nejad, Y., Hoffmann, E., Simon, J., Thüring, H. and Rüterjans, H., unpublished results). Although no

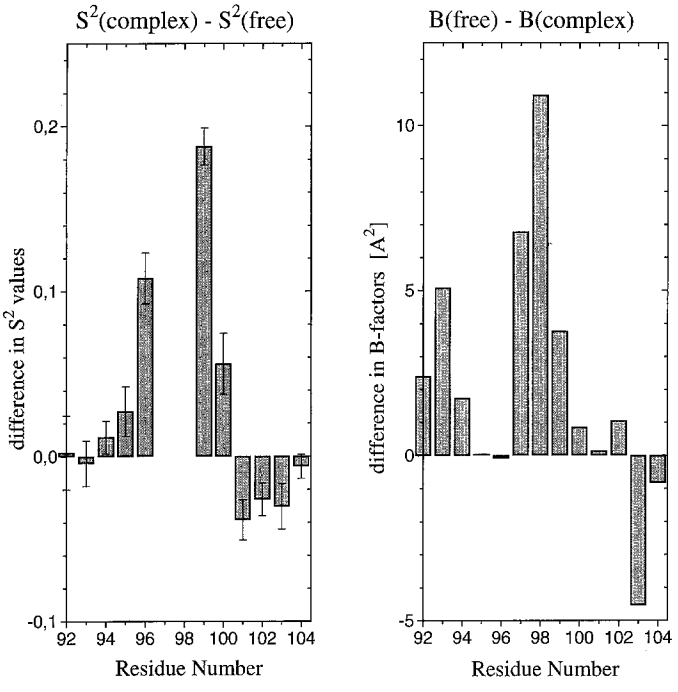

Fig. 8. Difference in S^2 values and in atomic B-factors in a complexed and free enzyme for amide nitrogens of the residues 92–104.

significant changes in the order parameter were observed for these residues upon inhibitor binding, as could be expected since they belong to the central β-sheet having a restricted local mobility, the corresponding values of the intrinsic rate R_{ex} are different.

For those residues that in both samples exhibit an influence of chemical exchange, the ratio of the R_{ex} values in the free enzyme and in the complex can be used to evaluate the differences in the chemical exchange rates, if the binding process is not accompanied by significant changes in the nitrogen chemical shift. Accordingly, for all residues listed in Table 1, except His^{40}, Lys^{41}, Asn^{43}, and Asn^{44}, the nitrogen chemical shift differences between corresponding resonances in both samples are less than 0.9 ppm. Neglecting these small chemical shift differences under identical experimental conditions to first order, the differences in the R_{ex} values for these residues may be safely attributed to changes in the respective exchange rates, see Eq. 7. In accordance with these arguments, the data shows a decreased exchange rate for residues Tyr^{42}, Tyr^{68}, Arg^{77}, and Val^{78}, whereas His^{27} exhibits an increased exchange rate relative to the free enzyme. In the case of Asn^{43}, the ^{15}N resonance shifts from 125.5 ppm in the free enzyme to 128.2 ppm in the ribonuclease T1 · 2'GMP complex. It is not clear if the observed difference in the R_{ex} values for this residue is due to changes in the exchange rate only. Note that, if one assumes a chemical shift difference of about 10 ppm ($2\delta = 2\pi$ 608.1 Hz for ^{15}N) between the two sites in Eq. 7, the exchange rate K should be about 10^6 s^{-1} in order to yield the observed values of R_{ex}.

Comparison of NMR microdynamic parameters and crystallographic B-factors

A comparison of the X-ray temperature factors derived for the backbone nitrogen nuclei with

the order parameter values obtained by the NMR approach reveals large qualitative coincidences in their distribution along the polypeptide chain (Figs. 6 and 7). Thus the high mobility of the loop regions II and V in free RNase T1 and that of loop II in the 2'GMP complex are obvious from both methods. Accordingly, the restriction of the local motion of the loop region participating in inhibitor binding is significant on the basis of X-ray analysis and NMR relaxation data. The differences in the $(1 - S^2)$ values obtained for both samples and those of the corresponding B-factors from the X-ray structures are depicted in Fig. 8, from which the changes of the microdynamic properties upon binding of 2'GMP in this region of the protein are obvious.

Despite the overall agreement concerning the dynamic properties of the molecules, differences may be seen between the two approaches with regard to the relative flexibility within regions of defined secondary structure. The NMR approach shows a higher intrinsic flexibility of the second strand of the central β-sheet (residues 56–61) in both investigated samples compared to that based on X-ray data (the distribution of the order parameters obtained for this region was more widely spread than that of the B-factors of the corresponding residues in both X-ray structures). Looking at the $(1 - S^2)$ distribution along the α-helix of RNase T1 (residues 13–29), a wide spread is observed for the first residues, while a significant decrease is observed for Tyr^{24}, which in this case is indicative of motional restriction or local anisotropic motion, whereas the B-factor distribution

TABLE 1
CHEMICAL EXCHANGE CONTRIBUTION TO THE OBSERVED TRANSVERSE RELAXATION RATES[a]

Residue	Free RNase T1 $R_{ex}(s^{-1})$	Complex RNase T1 · 2'GMP $R_{ex}(s^{-1})$	Ratio[b] K(free)/K(complex)
Tyr^{11}	1.31	[c]	
Asp^{15}	1.10	[c]	
Ser^{17}	2.31	[c]	
His^{27}	2.94	1.50	0.51
Val^{33}	[c]	1.18	
Ser^{37}	[c]	0.94	
His^{40}	2.09	[d]	
Lys^{41}	1.80	[d]	
Tyr^{42}	0.57	3.11	5.46
Asn^{43}	0.73	1.63	2.23
Asn^{44}	0.56	[e]	
Glu^{58}	0.79	[d]	
Tyr^{68}	0.90	1.18	1.31
Arg^{77}	0.37	1.20	3.24
Val^{78}	0.36	2.90	8.06
Asn^{84}	3.44	[c]	

[a] The values of R_{ex} were calculated using Eq. 5.

[b] The ratio of exchange constants was obtained via $R_{ex} \propto K^{-1}$ (Eq. 7).

[c] No noticeable increase of the transverse relaxation rate has been observed.

[d] No well-resolved cross peak has been observed, probably because of a large line broadening due to conformational exchange.

[e] The value of T_2 observed for Asp^{44} in the RNase T1 · 2'GMP complex, 89.8 ± 18.7 ms, indicates a considerable influence of chemical exchange processes, although an exact value for this contribution could not be obtained due to incomplete data.

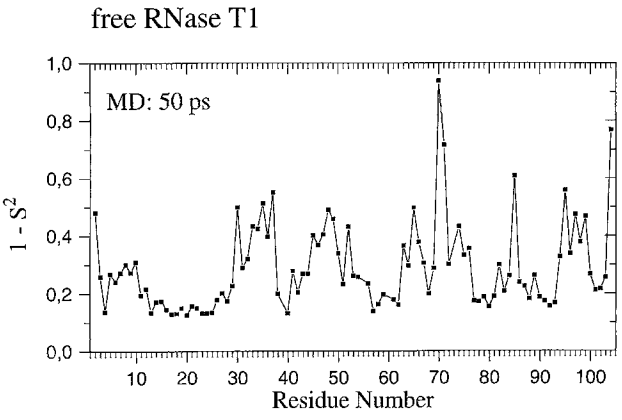

Fig. 9. Distribution of the $1 - S^2$ values obtained from the first 50 ps of a 1-ns molecular dynamics simulation of free RNase T1 (Fushman, D., Ohlenschläger, O. and Rüterjans, H., unpublished results).

is nearly uniform in this region of the protein. Recent NMR structure calculations (S. Pfeiffer, personal communication) for free RNase T1, as well as average structures from MD simulations of ribonuclease T1 mutants (Weisemann, R., unpublished results) show, in contrast to former X-ray crystallographic data, a slight bend of the α-helix towards the interior of the protein, which could indicate a bending motion, thus possibly explaining the differences in the mobility of the α-helix observed in the crystal state and in aqueous solution. These observations hold true for both the free enzyme and the inhibitor complex. Further investigations and a structure refinement of the RNase T1 solution structure are currently in progress in our laboratory.

Comparison of NMR microdynamic parameters and the results of MD simulations

To reach a better understanding of the picture of internal mobility of ribonuclease T1, solvent molecular dynamics simulations of both free enzyme and its 2'GMP-complex were carried out (Fushman, D., Ohlenschläger, O. and Rüterjans, H., unpublished results) in a water modelling environment by using the GROMOS library (van Gunsteren and Berendsen, 1987). Each simulation was extended to a trajectory length of 1 ns. The analysis showed that the picture of backbone NH-bond motion in the majority of cases is in agreement with the 'wobbling-in-a-cone' model, thus providing a clear relation between the values of the order parameter and the degree of spatial restriction of the local motion. To allow for a comparison with the results presented in this study, the relevant correlation functions of the backbone NH-bond reorientation were obtained and analysed in terms of the LS model. Comparison of the internal mobility observed in different time windows (of 50 ps and 1 ns length, each sampled with 1000 points) revealed a noticeable stability of the order parameter values for residues belonging to the structured regions of the protein backbone, whereas the parameters characterizing local motion in the unstructured parts of the latter were subject to some slow time–scale variations. The distribution of the $1 - S^2$ values derived from the first 50 ps of the MD simulation of free RNase T1 is presented in Fig. 9; a detailed report will be published elsewhere (Ohlenschläger, O., Fushman, D. and Rüterjans, H., unpublished results). Comparison of Figs. 6 and 9 shows a good agreement between the general behaviour of order parameters derived experimentally and from molecular dynamics simulations,

although the absolute values of S^2, especially in the loop regions, are markedly shorter when derived from computer-simulated dynamics. It is worthwhile mentioning that the results of the molecular dynamics simulation also show a restricted mobility of the loop 96–99 upon binding of the inhibitor.

CONCLUSIONS

In the present study, the fast and slow time–scale backbone dynamics of ribonuclease T1, as well as the changes of the microdynamic parameters of an enzyme upon binding of a competitive inhibitor, were investigated by using a consistent NMR methodology. From the S^2 values obtained for both the free RNase T1 and the RNase T1 · 2'GMP complex, it is evident that binding of the inhibitor changes the mobility of a certain region of the protein backbone, namely in the loop region between residues 93–99, being most prominent for the residues 95–99. The increase in the order parameter in this region for the RNase T1 · 2'GMP complex is accompanied by an increase in the T_1 and T_2 values of the corresponding residues in the free enzyme, as well as decreased NOE values in these cases, thus indicating a real motional restriction in the complexed enzyme compared to that of free RNase T1. From previous studies (Arni et al., 1988a, b), it is known that one of these residues, Asn^{98}, is directly involved in nucleotide binding by hydrogen bonding. Moreover, taking into account the decrease in the exchange rates of residues Asn^{43} and Tyr^{42} in the ribonuclease T1 · 2'GMP complex, residues which are also directly involved in the binding of the nucleotide, a more detailed, although not final, insight into the binding process may be gained. Significant small-scale mobility differences within regions of defined secondary structure were observed which may be attributed to conformational mobility of the α-helix and parts of the β-sheet of ribonuclease T1. The results obtained with our approach are in excellent general agreement with X-ray crystallographic data and molecular dynamics simulations, although the former is not able to differentiate between static disorder and thermal mobility, both contributing to the measured B-factors, and hence an X-ray approach seems to be less sensitive to subtle changes in the dynamics than the NMR approach, and the latter obviously suffers from the unsatisfying water model to be included in the calculations. It should be emphasized that the differences between the solution order parameters and the mobility data derived from either X-ray analysis or molecular dynamics simulation is attributed also to the fact that NMR-measured S^2 is sensitive only to motions on a time-scale faster than τ_c, whereas data obtained from both other techniques are not subject to this restriction.

A further analysis of the motional properties of the enzyme backbone by hydrogen exchange experiments and ^{15}N relaxation studies of other inhibitor complexes, as well as of the amino acid side chain atoms by ^{13}C NMR relaxation studies, which are currently in progress, will provide further data for construction of a general model of nucleotide binding by this enzyme.

ACKNOWLEDGEMENTS

We thank the Deutsche Forschungsgemeinschaft for a grant (RU-145/8-6). D.F. gratefully acknowledges a stipend from the Alexander von Humboldt Foundation. We thank Stefania Pfeiffer for making available the DIANA-obtained solution structures of RNase T1 prior to publication.

REFERENCES

Abragam, A. (1961) *The Principles of Nuclear Magnetism*, Clarendon Press, Oxford.

Anderson, P.W. (1954) *J. Phys. Soc. Japan*, **9**, 316–339.

Arata, Y., Kimura, S., Matsuo, H. and Narita, K. (1976) *Biochem. Biophys. Res. Commun.*, **73**, 133–140.

Arni, R., Heinemann, U., Maslowska, M., Tokuoda, R. and Saenger, W. (1988a) *Acta Cryst.*, **B 43**, 534–554.

Arni, R., Heinemann, U., Tokuoda, R. and Saenger, W. (1988b) *J. Biol. Chem.*, **263**, 15358–15368.

Barbato, G., Ikura, M., Kay, L.E., Pastor, R.W. and Bax, A. (1992) *Biochemistry*, **31**, 5269–5278.

Bloom, M., Reeves, L.W. and Wells, E.J. (1965) *J. Chem. Phys.*, **42**, 1615–1624.

Boyd, J., Hommel, U. and Campbell, I.D. (1990) *Chem. Phys. Lett.*, **175**, 477–482.

Boyd, J., Hommel, U. and Krishnan, V.V. (1991) *Chem. Phys. Lett.*, **187**, 317–324.

Carr, H.Y. and Purcell, E.M. (1954) *Phys. Rev.*, **94**, 630–632.

Chen, L.X.-Q., Longworth, J.W. and Fleming, G.R. (1987) *Biophys. J.*, **51**, 865–873.

Clore, G.M., Driscoll, P.C., Wingfield, P.T. and Gronenborn, A.M. (1990a) *Biochemistry*, **29**, 7387–7401.

Clore, G.M., Szabo, A., Bax, A., Kay, L.E., Driscoll, P.C. and Gronenborn, A.M. (1990b) *J. Am. Chem. Soc.*, **112**, 4989–4991.

Eftnik, M.R. (1983) *Biophys. J.*, **43**, 323–334.

Egami, F. and Sato, S. (1965) *Biochem. Zeitschrift*, **342**, 437–448.

Goldman, M. (1984) *J. Magn. Reson.*, **60**, 437–452.

Hakoshima, T., Toda, S., Sugio, S., Tomita, K.-I., Nishikawa, S., Morioka, H., Fuchimura, K., Kimura, T., Uesugi, S.-I., Ohtsuka, E. and Ikehaga, M. (1988) *Protein Eng.*, **2**, 55–61.

Heinemann, U. and Saenger, W. (1982) *Nature*, **299**, 27–31.

Heinemann, U. and Saenger, W. (1983) *J. Bimol. Struct. Dyn.*, **1**, 523–538.

Heinemann, U. and Hahn, U. (1989) In: *Topics in Molecular and Structural Biology*, Vol. 10, *Protein–Nucleic Acid Interactions* (Eds., Saenger, W. and Hahn, U.), Macmillan Press, London, pp. 111–134.

Hiyama, Y., Niu, C., Silverton, J.V., Bavaso, A. and Torchia, D.A. (1988) *J. Am. Chem. Soc.*, **110**, 2378–2383.

Hoffmann, E. and Rüterjans, H. (1988) *Eur. J. Biochem.*, **177**, 539–560.

James, D.R., Demmer, D.R., Steer, R.P. and Verall, R.E. (1985) *Biochemistry*, **24**, 5517–5526.

Kamath, U. and Shriver, J.W. (1989) *J. Biol. Chem.*, **264**, 5586–5592.

Kay, L.E., Torchia, D.A. and Bax, A. (1989) *Biochemistry*, **28**, 8972–8979.

Kay, L.E., Nicholson, L.K., Delaglio, F., Bax, A. and Torchia, D.A. (1992) *J. Magn. Reson.*, **97**, 359–375.

Lakowicz, J.R., Maliwal, B.P., Cherek, H. and Balter, A. (1983) *Biochemistry*, **22**, 1741–1752.

Lipari, G. and Szabo, A. (1982) *J. Am. Chem. Soc.*, **104**, 4546–4559; 4559–4570.

Martinez-Oyanedel, J., Choe, H., Heinemann, U. and Saenger, W. (1991) *J. Mol. Biol.*, **222**, 335–352.

Meiboom, S. and Gill, D. (1958) *Rev. Sci. Instrum.*, **29**, 688–691.

Nicholson, L.K., Kay, L.E., Baldsseri, D.M., Arango, J., Young, P.E., Bax, A. and Torchia, D.A. (1991) *Biochemistry*, **31**, 5253–5263.

Palmer III, A.G., Skelton, N.J., Chazin, W.J., Wright, P.E. and Rance, M. (1992) *Mol. Phys.*, **75**, 699–711.

Press, W.H., Flannery, B.P., Teukolsky, S.A. and Vetterling, W.T. (1988) *Numerical Recipes*, Cambridge University Press, Cambridge.

Quaas, R., Grunert, H.-P., Kimura, M. and Hahn, U. (1988a), *Nucleosides Nucleotides*, **7**, 619–623.

Quaas, R., McKeown, Y., Stanssens, P., Frank, R., Blöcker, H. and Hahn, U. (1988b), *Eur. J. Biochem.*, **173**, 617–622.

Redfield, C., Boyd, J., Smith, L.J., Smith, R.A.G. and Dobson, C.M. (1992) *Biochemistry* **31**, 10431–10437.

Rüterjans, H., Hoffmann, E., Schmidt, J. and Simon, J. (1987) In *Metabolism and Enzymology of Nucleic Acids Including Gene Manipulations*, Vol. 6 (Eds., Zhelinka, J. and Balan, J.), Slovak Academy of Sciences, Bratislava, pp. 81–96.

Schmidt, J.M. (1990) Ph.D. Thesis, Frankfurt.

Schmidt, J.M., Thüring, H., Werner, A., Rüterjans, H., Quaas, R. and Hahn, U. (1991) *Eur. J. Biochem.*, **197**, 643–653.

Steyaert, J., Haikal, A.F., Wyns, L. and Stanssens, P. (1991) *Biochemistry*, **30**, 8666–8670.

Sugio, S., Oka, K., Ohishi, T., Tomita, K., Heinemann, U. and Saenger, W. (1985) *FEBS Lett.*, **183**, 115–118.

Sugio, S., Amisaki, T., Ohishi, H. and Tomita, K. (1988) *J. Biochem.*, **103**, 354–366.

Takahashi, K., Stein, W.H. and Moore, S. (1967) *J. Biol. Chem.*, **242**, 4682–4690.

Takahashi, K. (1970) *J. Biochem.*, **68**, 659–664.

Takahashi, K. (1976) *J. Biochem.*, **80**, 1267–1275.

Van Gunsteren, W.F. and Berendsen, H.J.C. (1987) *Groningen Molecular Simulation (GROMOS) Library Manual*, Biomos, University of Groningen, Groningen.